Research Article

Proteome dynamics in persisting and resuscitating bacterial cells

Maja Semanjski[1*], Fabio Gratani[1*], Till Englert[1], Viktor Beke[1], Nicolas Nalpas[1], Elsa Germain[2,3], Kenn Gerdes[2#], Boris Macek[1#]

1) Quantitative Proteomics, Interfaculty Institute of Cell Biology, Faculty of Science, University of Tuebingen, Germany

2) Centre for Bacterial Stress Response and Persistence, Section for Functional Genomics, Department of Biology, University of Copenhagen

3) Laboratoire de Chimie Bacterienne, CNRS, IMM, 31 chemin Joseph Aiguier 13009 Marseille, France

[*]**Equal contribution**

[#]**Corresponding Authors:**

Prof. Boris Macek
Quantitative Proteomics &
Proteome Center Tuebingen
Interfaculty Institute for Cell Biology
Department of Biology
University of Tuebingen
Auf der Morgenstelle 15
72076 Tuebingen
Germany
Phone: +49 7071 29 70556
Fax: +49 7071 29 5779
E-mail: boris.macek@uni-tuebingen.de

Prof. Kenn Gerdes
Centre for Bacterial Stress Response and Persistence
Section for Functional Genomics
Department of Biology
University of Copenhagen
Ole Maaløes Vej 5
DK-2200 Copenhagen N
Denmark
Phone: +45 35 33 02 19
Fax: +45 51 82 70 57
E-Mail: kenn.gerdes5@gmail.com

Abstract

Bacterial persister cells become transiently tolerant to antibiotics by restraining their growth and metabolic activity. Detailed molecular characterization of bacterial persistence is hindered by low count of persisting cells and the need for their isolation. Here we used sustained addition of stable isotope-labeled lysine to selectively label the proteome of *hipA*-induced persisting and *hipB*-induced resuscitating *E. coli* cells in minimal medium after antibiotic treatment. Time-resolved, 24-hour measurement of label incorporation allowed detection of over 500 newly synthetized proteins in persister cells, demonstrating low but widespread protein synthesis. Many essential proteins were newly synthesized and several ribosome-associated proteins showed unusually high synthesis levels, pointing to their roles in maintenance of persistence. At the onset of resuscitation, cells synthesized ABC transporters, restored translation machinery and resumed metabolism by inducing glycolysis and biosynthesis of amino acids. This dataset provides an unprecedented insight into the processes governing persistence and resuscitation of bacterial cells.

Introduction

Antibiotic resistance is an acute health problem. Many bacteria are categorized as serious threats representing a considerable clinical and financial burden (Brauner et al., 2016; Ventola, 2015). In addition to resistance, bacteria also possess an elusive innate strategy, termed persistence, that enables them to tolerate antibiotics without acquiring genetic changes (Van den Bergh et al., 2017). Persisters are defined as phenotypic variants of bacterial cells that become transiently tolerant to antibiotics by restraining their growth and entering a dormant-like state (Balaban et al., 2004; Lewis, 2010). Persistence is exhibited within a subpopulation of genetically uniform cells, a phenomenon present in all bacteria tested so far (Balaban, 2011; Balaban et al., 2019). While bactericidal antibiotics typically require actively growing cells to exploit their function, persister cells are slowly replicating which makes them tolerant to the lethal action of antimicrobials. In addition to slow growth, the persister phenotype is also associated with very low metabolic activity (Amato et al., 2014), although persisters are not entirely metabolically inactive (Helaine et al., 2014).

Persistence can be induced by toxin-antitoxin (TA) modules that usually consist of two genes: one encoding a toxin that inhibits cell growth, and another encoding an antitoxin that inhibits toxin activity (Harms et al., 2016; Page and Peti, 2016). While the product of the toxin gene is always a protein that interferes with essential cellular functions, antitoxin genes encode either small proteins or noncoding RNAs (Page and Peti, 2016). Low counts of persister cells in bacterial cultures necessitate application of elaborate protocols for their isolation (Canas-Duarte et al., 2014; Radzikowski et al., 2017; Rowe et al., 2016), making detailed exploration of their unperturbed molecular processes a challenging task.

Here we used an in-vitro model of bacterial persistence based on overexpression of the toxin-antitoxin (TA) system *hipA*/*hipB* (Germain et al., 2013; Semanjski et al., 2018) to devise a generic method for temporal analysis of protein synthesis during toxin-induced persistence and antitoxin-mediated

resuscitation. We reasoned that prolonged antibiotic treatment of HipA-induced *E. coli* cells, which results in a mixture of dead (lysed) and living (persisting) cells, can be coupled with sustained addition of stable isotope-labeled amino acid directly to the culture. As only the living (persisting) cells are capable of incorporating the label, and the label mass shift can be easily resolved in a mass spectrometer, this approach can be used to selectively label and detect newly synthesized persister proteins in the high background of proteins originating from dead cells. Similar strategies, termed "pulsed" or "dynamic" stable isotope labeling by amino acids in cell culture (SILAC), have previously been used to analyze protein turnover in eukaryotic (Doherty et al., 2009; Schwanhäusser et al., 2011) and prokaryotic cells (Chua et al., 2016; Spanka et al., 2019).

Results and Discussion

HipA-induced persister cells show low but measurable protein synthesis

To test applicability of our approach, we first increased the number of persister cells growing in minimal medium by ectopically inducing *hipA* in *E. coli* MG1655. Three hours after HipA-induced growth inhibition, we treated the culture with ampicillin to lyse non-persister cells. During ampicillin treatment, we repressed expression of *hipA* by addition of glucose to ensure steady state conditions independent of the constant HipA overproduction. Twenty hours after ampicillin treatment, we added $^{15}N2^{13}C6$-lysine (Lys8) to the culture; this time point was sufficient to eradicate sensitive cells and achieve a steady state of persistence, as demonstrated by approximately 1000-fold higher count of colony-forming units (CFUs) in *hipA*-induced strain compared to the empty vector (**Supplementary Figure 1A,B**). After introduction of the Lys8 label, we harvested the culture aliquots by brief centrifugation to pellet intact cells in three biological replicates and multiple time points ranging from 10 minutes to 24 hours (**Figure 1A**). In this experimental setup, only living (persister) cells incorporated Lys8, which enabled persister-specific

detection of newly synthesized proteins, temporal quantification of protein abundance and estimation of protein half-lives (**Supplementary Figure 1C, Supplementary Table S1**). The number of identified proteins across time points was consistent, with 1,993 proteins identified on average in each time point (**Supplementary Figure 1D**). Remarkably, up to 581 proteins have partially incorporated the Lys8 label and were reproducibly quantifiable in the high background of Lys0-labeled proteins originating from dead cells (**Supplementary Figure 1D,E**). Due to HipA-mediated inhibition of cell growth, incorporation of Lys8 in these proteins was only partial and expectedly low; 24 hours after the start of labeling the average intensity of all heavy labeled signals amounted to only 8.64% of the total ion intensity (**Figure 1B**). Nevertheless, the measurable label incorporation was indicative of protein synthesis in persisting cells and was in agreement with previous studies (Pu et al., 2016; Spanka et al., 2019; Sulaiman et al., 2018). The low level of label incorporation reflected the low turnover rates and long half-lifes of proteins in persisting cells. Estimation of protein half-lifes from the measured H/L ratios, as described previously (Schwanhäusser et al., 2011), revealed that the median protein half-life during persistence was longer than 250 hours (**Supplementary Figure 1F, Supplementary Table S1**). This, however, is only an estimate, since our measurement window (24h) was significantly shorter than the actual protein half-life and our calculation was based on the assumption of complete cell cycle arrest. This experiment demonstrated that it is possible to partially label and directly detect newly synthesized proteins of persister cells enriched by toxin overproduction and antibiotic treatment. All measured proteins and their ratios are listed in the **Supplementary Table S2** and can be browsed online under https://pctsee.pct.uni-tuebingen.de.

Persisting bacteria produce proteins needed for essential cellular processes

For further data analysis, the time points over the entire 24-hour course of persistence were collapsed into six time bins and proteins were ranked based on their H/L ratios. Gene Ontology (GO) analysis of all

newly synthesized proteins showed that proteins involved in translation, glycolysis, protein targeting, redox homeostasis and tricarboxylic-acid cycle were significantly enriched (p < 0.01) **(Supplementary Table S3)**. Importantly, almost all ribosomal proteins were overrepresented among top 25% proteins that exhibited relatively high label incorporation across all time points (p = 1.67E-15). In contrast, proteins with lower label incorporation (bottom 25%) participate mainly in the metabolic pathways such as biosynthesis of amino acids and other metabolites (**Figure 1C**). Interestingly, enzymes involved in protein degradation, including degradation of antitoxins necessary to maintain an optimal toxin/antitoxin ratio during persistence, also exhibited higher label incorporation. They included several proteases (Lon, HslU, HslV and HtpX), as well as the specificity components of the Clp protease (ClpA and ClpX, but not ClpP), implying that protein degradation is active during persistence (**Figure 1D**). Two antitoxins, PrlF and MqsA, as well as several heat and cold shock proteins involved in stress response, also showed Lys8 incorporation. Furthermore, proteins involved in transcription, such as the ribonucleases RNase R (Rnr) and RNase III (Rnc) required for RNA processing and turnover, including the RNA polymerase sigma factor RpoD, were also detected as newly synthesized, as were several translation regulatory proteins essential for the start of protein synthesis, such as translation initiation factors IF-1 and IF-3 (InfA and InfC) (**Figure 1E**). Several chaperones were detected as newly synthesized during persistence (Error! Reference source not found.**F**), suggesting that they may be required for the maintenance of proteome homeostasis, either by enabling correct folding of misfolded client proteins or by targeting unfolded (or aggregated) proteins for degradation. Among them were DnaK, DnaJ and ClpB, that were previously connected to persistence (Hansen et al., 2008; Keren et al., 2004). Moreover, one of the most important DNA repair proteins RecA was identified as newly synthesized in our study, which is in agreement with a previous report that SOS response genes are expressed during persistence due to inhibited DNA replication (Keren et al., 2004). These results indicate that persister cells perform active translation and produce proteins that are needed

for essential cellular processes. In fact, out of 299 essential gene products in *E. coli*, 159 incorporated the label during persistence (**Supplementary Table S4**).

Ribosome-associated proteins RaiA and Sra show elevated synthesis levels in persisting cells

Consistent with the slow growth attributed to persister cells, proteins required for cell division (FtsH, FtsZ, FtsY and ZipA) were either not detected or displayed very low label incorporation in our data set, suggesting that residual cell growth is still present, but is extremely slow. Accordingly, chemotaxis-related proteins that are important for cell motility were not identified, which supports the absence of the cell movement during persistence. The low abundance of newly synthesized proteins involved in metabolism, mainly in biosynthesis of amino acids and primary carbon metabolism, demonstrated that major energy-generating pathways are active in our model of persistence, but their activity is very low (Error! Reference source not found.). In contrast to reduced metabolism and cell division, we found that ribosomal proteins and general stress response-related proteins were incorporating the Lys8 label to a higher extent during persistence.

Regulation of ribosome function is known to have a key role in bacterial persistence (Prossliner et al., 2018); therefore, we next analyzed relative abundance and label incorporation of all detected ribosomal proteins, as well as ribosome-associated hibernation and stationary phase factors proposed to modulate ribosomal activity, such as EttA, RaiA, ElaB, YqjD and Sra (Gohara and Yap, 2018; Prossliner et al., 2018; Yoshida and Wada, 2014). In persisting cells, measured rates of label incorporation and relative abundances of most ribosomal proteins were relatively high (**Figure 2A**). Of hibernation factors, only RaiA was detected as newly synthesized at a relatively high rate, pointing to its potential role as a major factor in active maintenance of ribosome hibernation during persistence. Intriguingly, the stationary phase ribosome associated factor Sra showed an even higher label incorporation rate and is therefore likely to

be involved in the maintenance of ribosome hibernation (**Figure 2A**). Importantly, the level of newly synthesized GTPase HflX, proposed to mediate activation of hibernating ribosome dimers (Zhang et al., 2015), was not detectable during persistence. Strikingly, the overall abundance of newly synthesized hibernation factors (predominantly RaiA), estimated using intensity-based absolute quantification (iBAQ) of the heavy isotope channel, were about 100 times higher than the level of all newly synthesized ribosomal proteins combined (**Figure 2B, Supplementary Table S5**).

Ribosome-associated proteins RaiA and Sra are involved in antibiotic tolerance

To test whether ribosome-associated proteins Sra and RaiA influence HipA-induced persistence and antibiotic tolerance, we ectopically induced *hipA* in *E. coli sra* and/or *raiA* deletion strains in the log phase for one hour and treated the cultures with ciprofloxacin. Already 60 minutes after addition of antibiotic, the CFU count of the *hipA*-expressing *sra* and *raiA* deletion mutants was lower compared to the *hipA*-expressing WT, pointing to a lower tolerance of these strains to ciprofloxacin (**Figure 2C**). This effect was even more pronounced 120 minutes after addition of antibiotic, with the CFU count about 10 times lower than in the *hipA*-expressing WT. Of note, the CFU level in the *raiA* deletion strain seemed to be relatively stable over time, whereas the *sra* deletion strain showed a sharper drop in viability. This experiment strongly suggested a role of ribosome-associated proteins RaiA and Sra in active maintenance of bacterial persistence and antibiotic tolerance.

HipB-induction leads to rapid resuscitation and incorporation of the Lys8 label

We next applied our approach to study proteins produced upon induction of resuscitation. As in the first experiment, we increased the number of persister cells by ectopically inducing *hipA* in minimal medium supplemented with Lys0 and treated the culture with a high dose of ampicillin. During ampicillin

treatment, we repressed expression of *hipA* by addition of glucose to ensure steady state conditions independent of any HipA overproduction. To trigger resuscitation, we removed ampicillin, Lys0 and cellular extract of lysed cells by gentle filtration and added fresh minimal medium containing IPTG to induce transcription of antitoxin *hipB*. The medium also contained "heavy" lysine (Lys8) for metabolic labeling of resuscitating cells. Filtered cultures exposed to the fresh, IPTG-containing medium resumed growth, whereas unfiltered control cultures did not (**Supplementary Figure 2A**), demonstrating that resuscitation was driven by *hipB* induction. The resuscitating culture was harvested in three biological replicates and 20 time points (**Figure 3A**). Incorporation of Lys8 in resuscitating cells followed the shape of the growth curve and saturated at average 94.6 % (**Figure 3B**). Already 30 minutes after induction of resuscitation, more than 100 proteins incorporated the Lys8 label and could be quantified. Although the median of Lys8 incorporation during the first four hours was low (< 8 %), presence of outliers indicated that a subset of proteins incorporated the label faster than others and are therefore likely to play a role in resuscitation. On average, 1,880 proteins were identified at an estimated FDR of 1.3% (**Supplementary Figure 2B**). The three biological replicates showed good reproducibility of measured protein SILAC ratios across all time points (**Supplementary Figure 2C; Supplementary Table S6**).

To analyze processes occurring early during resuscitation, we considered time points from the first eight hours of *hipB* induction, in which the optical density doubled. Measured protein ratios were collapsed into five time bins and proteins were ranked based on their H/L ratio within each time bin. According to the KEGG pathway enrichment analysis, proteins exhibiting high label incorporation (top 25%) during the entire eight-hour course of resuscitation are involved mainly in the biosynthesis and transport of amino acids, such as arginine and cysteine, as well as in alanine, aspartate and glutamate metabolism (p-value < 0.05). Conversely, proteins with a low label incorporation (bottom 25%) are constituents of the citric acid cycle, amino sugar and nucleotide sugar metabolism (**Figure 3C**). Altogether, this implies that resuscitating bacteria are predominantly synthetizing enyzmes for anabolic pathways to produce building blocks for

cell growth. Proteins involved in catabolic pathways that consume metabolites to release energy are synthesized at a slower rate compared to all quantified proteins. This is in agreement with our experimental design, as we were resuscitating cells with glucose as carbon source. Therefore, most energy was derived from glucose catabolism (glycolysis), not from the catabolism of other metabolites.

Onset of resuscitation is marked by restoration of glycolysis and translation machinery

To identify proteins that are potentially regulating the switch from persistence to resuscitation, the first time bin (10 – 30min) after induction of *hipB* was analyzed in more detail. GO enrichment analysis revealed that 43 out of 153 quantified proteins take part in translation (p = 2.75E-27), out of which 42 are ribosomal proteins and one is the stationary-phase-induced ribosome-associated protein Sra (**Supplementary Table S7,8**). Glycolysis pathway, stress response and protein folding were also significantly enriched. This implies that, at the very onset of resuscitation, cells restored almost the entire translation machinery and restarted their metabolism by inducing glycolysis to convert glucose from the fresh medium into energy used for regrowth (**Supplementary Table S8)**. Of note, we recently made a similar observation in resuscitation of chlorotic cyanobacteria (Spat et al., 2018), pointing to the existence of a common program for awakening of dormant-like cells. Two chaperones (DnaK and GroL) and transcription-related proteins (Rho, DeaD and Pnp) that are involved in RNA metabolism and degradation, were newly synthesized during early response, possibly regulating transcription of specific genes. Because these proteins were also detected to be synthesized during persistence, it is possible that the processes common to persistence are still active during the initial phase of the pulse-labeling. The delay in the wake-up from dormancy was observed previously and depends on several factors, such as the composition of the outgrowth medium or the frequency of persister cells (Jõers et al., 2010; Varik et al., 2016). Several proteins showed unusually high label incorporation in the first 30 minutes after induction of resuscitation.

As expected, among them was HipB antitoxin that was induced from the plasmid and therefore served as a positive control. Other proteins participate in various processes, such as the ribonucleotide monophosphatase NagD that dephosphorylates a wide range of (deoxy)ribonucleoside phosphates, or the S-formylglutathione hydrolase FrmB, which converts S-formylglutathione into formate and glutathione to detoxify formaldehyde that can otherwise chemically modify DNA and proteins (Denby et al., 2016). Among them were also several proteins known to play a role in persistence, such as the ATP-dependent Clp protease subunit ClpA that directs the ClpAP protease to specific substrates for their degradation (Battesti et al., 2011; Gottesman et al., 1998) and the RNA polymerase sigma factors RpoS and RpoD (**Figure 3C**). RpoS is important for transcriptional reprograming of many genes that are mainly involved in the metabolism and stress response (Battesti et al., 2011), whereas RpoD preferentially induces transcription of genes associated with fast growth, such as ribosomal proteins (Maciąg et al., 2011), which is in agreement with our findings (see below). Considering that RpoD was also detected during persistence, it can be assumed that it might have a dual role during both processes. Moreover, several other proteins were rapidly synthesized during early resuscitation, such as the NemA, which reduces N-ethylmaleimide that inhibits growth by modifying cysteine residues of cellular proteins (Miura et al., 1997). NamA is also known to degrade toxic compounds to use them as a source of nitrogen (Umezawa et al., 2008)(**Supplementary Figure S3**).

Resuscitation is a concerted and tightly regulated biological process

To get a global insight into processes occurring during resuscitation, we performed statistical enrichment analysis of KEGG and GO-annotated functions in each of the five time bins. Functions related to the ribosome and protein biosynthesis were significantly enriched in all time bins, demonstrating that translation is the key process that dominates resuscitation. In addition, the following protein functions

were overrepresented: bin 1 (10-30 min): glycolysis and chaperone-mediated protein folding; bin 2 (45-90 min): glycolysis and aminoacyl-tRNA synthetase; bin 3 (2-3h): biosynthesis of antibiotics and amino acids; bin 4 (4-5h) and bin 5 (6-8h): biosynthesis of amino acids, antibiotics and carbon metabolism (**Supplementary Table S8**). For 1663 proteins we were able to measure label incorporation over all 21 measured time points. Unsupervised clustering of their temporal profiles revealed eight distinct clusters that differed markedly in the rate of label incorporation, estimated by the average time needed to incorporate 50% of the label (**Supplementary Figure 4, Supplementary Table S9**). Among proteins with fast label incorporation, functions such as "ABC transporters" and "arginine biosynthetic process" were overrepresented ("early functions"). They were followed by protein clusters enriched in diverse metabolic pathways and protein biosynthesis ("intermediate functions"). Proteins with the slowest label incorporation were predominantly involved in various catabolic processes; these "late functions" most likely do not play a role in resuscitation, but may be of importance in transition to stationary phase that was also covered in our analysis. Combined, this analysis revealed that resuscitation is a tightly regulated biological process that starts with activation of protein translation and synthesis of transporters needed to import nutrients and building blocks for protein biosynthesis.

Ribosomal hibernation factor HflX is induced in resuscitating cells

Almost all detected ribosomal proteins showed synchronized label incorporation during resuscitation (**Figure 4A**). Two notable exemptions were the ribosomal proteins L31-type B and L36-2, that showed markedly higher label incorporation compared to other ribosomal proteins. Approximately 10 hours after *hipB* induction the levels of these two proteins surpassed the levels of their paralogs L31 and L36, pointing to a rearrangement of the large ribosome subunit at the entry of the stationary phase (**Supplementary Figure 2D**). This observation, which was recently reported in another study (Lilleorg et al., 2019), demonstrates the potential of the used approach to detect dynamics of protein complexes in a rapidly

changing biological system. Resuscitation was also marked by induction of HflX that correlated with increased synthesis of ribosomal (and other) proteins (**Figure 4B, Supplementary Table S10**). Of note, the synthesis of other hibernation and stress factors such as RaiA and Sra did not diminish during resuscitation; however, as opposed to persisting cells, they were not in excess compared to newly synthesized ribosomal proteins.

Limitations of the applied experimental strategy

Molecular investigation of persister cells is challenging and our approach is not free of experimental bias. We used the lytic antibiotic ampicillin to enrich for persisters by physically eliminating sensitive cells; however, the fraction of dead cells cellwith intact membrane was still substantial. Therefore, a limitation of our approach is the contamination of the persister cells with the unlabeled pool of proteins that originate from dead cells. Although these proteins can be easily discriminated according to the mass shift of their label, the resulting complexity of the mixture, in combination with a limited dynamic range of mass spectrometric detection, has lead to decreased sensitivity of the measurements and lower proteome coverage compared to a usual shotgun proteomics experiment. This issue could be circumvented by an additional enrichment step to isolate persister cells from the batch culture, for example using long enzymatic treatment that targets the cell membrane (Cañas-Duarte et al., 2014) or centrifugation (Pu et al., 2016). However, such approaches would impose a significant stress to the cells, resulting in proteome changes that could finally lead to data misinterpretation. We cannot exclude that even gentle filtration of the bacterial culture, performed to induce resuscitation and introduce the Lys8 label, introduced some stress to the cell. The alternative could be persister isolation using flow cytometry based on GFP expression from plasmid carrying specific promoters of genes associated with dormancy, as reported previously (Schumacher et al., 2015; Shah et al., 2006).

Ideally, the enrichment should not be performed on living cells, but rather on isolated proteins that incorporated the label. For this, approaches based on click-chemistry could be used, such as the metabolic labeling with methionine analogue L-azidohomoalanine (AHA) with subsequent attachment of an affinity tag to the reactive azide-group and enrichment of the labeled proteins by affinity chromatography (Dieterich et al., 2007). However, in our experience the application of AHA interferes significantly with translation and causes severe growth defects, which is not compatible with our study.

Application of labeled amino acids to study protein synthesis and turnover is also exposed to technical bias, which mainly concerns a limited dynamic range of detection in a mass spectrometer. This means that very low level of label incorporation will not be detected in a high background of MS signals originating from unlabeled peptides. A further complication concerns the recycling of amino acids released from degradation of pre-existing proteins into the medium. This causes a dilution of labeled amino acid pool with unlabeled amino acids and results in apparently lower turnover rates that cannot truly describe actual values. These values can be corrected using a recycling factor that can be calculated by measuring label incorporation in partially labeled missed cleaved peptides (Schwanhäusser et al., 2011). Although these issues may influence the overall sensitivity and accurate estimation of individual protein turnover rates, we do not expect that they lead to a false detection of the newly synthesized proteins.

Materials and Methods

Bacterial strains and plasmids

E. coli strains and plasmids used in this study are listed in the **Table 1**. Due to a high toxicity of HipA protein, *hipA* gene was cloned into the expression plasmids together with a Shine-Dalgarno sequence in which the spacer between the Shine-Dalgarno and the start codon was changed to decrease the translation efficiency of HipA (Ringquist et al., 1992). In Table S1, sd8 specifies a consensus sequence AAGGAA with a spacer of eight nucleotides to the GTG start codon. Oligonucleotides used are listed in the **Table 2**.

The *lysA::FRT::Kan::FRT* deletion strain from the Keio collection (Baba et al., 2006) was P1 transduced into MG1655. The resulting mutation was verified by PCR diagnostics using primers EG239 and EG240 and then transformed with pCP20 to induce the flippase to flip out the Kan^R gene, resulting in MG1655 *lysA*::*FRT* mutant. The *sra::FRT::Kan::FRT* and The *sra::FRT::Kan::FRT* deletion strains from the Keio collection (Baba et al., 2006) was P1 transduced into MG1655.

Plasmid pEG220 was constructed to change the kanamycin cassette of the expression plasmid pNDM220 (Gotfredsen and Gerdes, 1998) to ampicillin. The ampicillin cassette has been amplified with primer EG287 and EG288 from pKD4. Then, DY331 strain has been electroporated with PCR fragment following the procedure from D.Court's laboratory (https://redrecombineering.ncifcrf.gov/protocols/). The correct insertion of the ampicillin cassette has been verified using primer EM67 and EM68 matching in the insertion in the pNDM220. Then, the kanamycin cassette and the surrounding region of the newly constructed pEG220 were sequenced using primers EM67 and EM68.

For construction of plasmid pEG220::*hipB*, *hipB* coding region with an optimized Shine Dalgarno was PCR amplified using primer EM172 and EM173, the resulting DNA fragment digested with BamHI and EcoRI and ligated in pEG220 digested with the same enzymes.

Table 1. List of bacterial strains and plasmids

Strains/Plasmids	Genotype	Source
Strains		
MG1655	Wild-type *E. coli*	(Guyer et al., 1981)
ΔlysA	MG1655 *ΔlysA::FRT* P1 transduction from BW25113 *lysA::FRT::aphA::FRT* (KEIO collection) into MG1655 and flipped out.	This work
sra::kana^R	MG1655 *sra::FRT::aphA::FRT* P1 transduction from BW25113 *sra::FRT::aphA::FRT* (KEIO collection) into MG1655	This work
raiA::kana^R	MG1655 *raiA:: ::FRT::aphA::FRT* P1 transduction from BW25113 *raiA:: ::FRT::aphA::FRT* (KEIO collection) into MG1655	This work
Plasmids		
pBAD33	p15 derived expression plasmid, *cat*, *araC*, P_{BAD} promoter, Cm^R	(Guzman et al., 1995)
pNDM220	R1 derived expression plasmid, $p_{A1/O4/O3}$ (p_{lac}), *lacI*^{q}, *aphA* (Km^R)	(Gotfredsen and Gerdes, 1998)
pBAD33::*hipA* (pEG5)	pBAD33 P_{BAD}:: sd8 *gtg hipA*	(Germain et al., 2013)
pEG220::*hipB*	pEG220 P_{lac}:: sdopt::*hipB*, Km^R	This work

Table 2. List of DNA oligonucleotides

Primers	Sequence 5' to 3'
EG287	ttaaaaatgaagttttaaatcaatctaaagtatatatgagtaaacttggtctgacagttatatggacagcaagcgaaccg
EG288	aggtggcacttttcggggaaatgtgcgcggaacccctatttgtttatttttctaaatacatcagaagaactcgtcaagaag
EM67	gactgggcacaacagacaat
EM68	ggatgatctggacgaagagc
EG239	catagactcgacataaatcg
EM172	cccccggatccgtcgactcaaggagttttataaatgatgagctttcagaagatcta
EM173	cccccgaattcttaccactccagattttgctgtt
raiA.del.KO-f	agacgggaagacaagaggt
raiA.del.KO-r	gcgttggcgatacactca
sra.del.KO-f	cgcaggcaatggtgtttaa
sra.del.KO-r	ctacggcgatgttgtcct

Persistence analysis

Pre-cultures were grown overnight in LB medium (Luria-Broth) supplemented with 0.4% (w/v) glucose, 25 µg/ml chloramphenicol for maintenance of pBAD33::*hipA* plasmid and, for *sra::kana*^{r} and *raiA::kana*^{r}, additional 50 µg/ml kanamycin. Day cultures were inoculated at OD_{600nm} of 0.08; at OD_{600nm} of 0.3 HipA was induced with 0.2 % (w/v) L-(+)-arabinose for 1h, followed by 1 µg/ml ciprofloxacin. Cells were harvested at desired time points, pellets were washed with phosphate-saline buffer (PBS), serially diluted and spotted on LB-agar plates supplemented with 0.4% (w/v) glucose. Expermiment was performed in triplicates. Statistical analysis was performed using Prism 6 (GraphPad), via two-way ANOVA correcting the multiple comparison with Tukey test and confidence level set at 95%.

P1 phage preparation and transduction

Pre-culture were inculated in LB broth supplemented with 50 µg/ml of kanamycin. For lysate preparation, the overnight donor culture was diluted 1:100 into 5 ml of 0.2% (w/v) glucose and 5 mM CaCl2 and incubated 30 to 45 min at 37°C with shaking. 100 µl of P1 phage stock were added to the growing culture and incubated, with shaking, until the culture lysed (~3 hr). To complete cell lysis few drops of $CHCl_3$ were added to the shaking culture. The culture was pelleted via centrifugation for 10 min at ~9200 × g at 4°C and the supernatant containing the phages was filtered over a 0.45 µm sterile filter. For P1 transduction, *E. coli* recipient strain was inoculated in 5ml LB broth overnight at 37° C. The following day, 1.5 ml of the cell culture was pelleted by centrifugation for two minutes at maximum speed at room temperature and the pellet was resuspended in P1 salt solution (10 mM $CaCl_2$, 5 mM $MgSO_4$), at half of the original volume. 100 µl of the cell/P1 mixture was mixed with different amounts of the desired P1 lysate (1, 10, and 100 µl) and the phage was allowed to adsorb for 30 min at room temperature. One mililiter LB broth plus 200 µl of 1 M sodium citrate was added to the cell/pahge mix and incubated for 1 h at 37° C. Coltures were

then centrifuged, supernatants removed and the pellets resuspended in LB medium. Resuspended cells were plated on LB agar plates supplemented with 50 µg/ml kanamicyn. Single colonies were streaked on fresh selective plates and confirmed by PCR.

Cell growth and SILAC labeling

Cells were grown in 100 ml of M9 minimal medium (50 mM Na_2HPO_4, 22 mM KH_2PO_4, 8.6 mM NaCl, 18.7 mM NH_4Cl, 1 mM $MgSO_4$, 0.1 mM $CaCal_2$, 0.0001% (w/v) thiamine) supplemented with 0.4% (v/v) glycerol, 25 µg/ml chloramphenicol for maintenance of pBAD33::*hipA* plasmid and 50 µg/ml kanamycin for maintenance of pEG220::*hipB* plasmid. Cultures were grown in batch at 37 ˚C shaking at 200 rpm. Pre-cultures were grown for 20 hours in M9 medium supplemented with 0.4% (w/v) D-(+)-glucose to repress the P_{BAD} promoter. Main cultures were grown starting from OD_{600nm} of 0.01 – 0.02 in M9 medium without glucose. For HipA-induced persistence, wild type *E. coli* K-12 MG1655 strain was used. The expression of *hipA* was induced with 0.2% (w/v) L-(+)-arabinose at OD_{600nm} of ≈0.4. After 3 hours of *hipA* expression, cultures were treated with 100 µg/ml ampicillin for 19 - 22 hours to kill non-persister cells and 0.4% glucose to repress transcription of the P_{BAD}*::hipA* promoter fusion. A pulse of 0.025% (w/v) stable isotope-labeled lysine derivative $^{13}C_6{}^{15}N_2$ L-lysine (“heavy” lysine, Lys8, K8, Cambridge Isotope Laboratories) was then added in the presence of ampicillin and 1 – 2 mL of cultures were harvested in intermittent time intervals (10min - 24h) by centrifugation at 4 ˚C. A time point before the pulse of Lys8 (0h) was harvested as a control. For the resuscitation experiment, an MG1655 derived strain lacking *lysA* (*ΔlysA*) was used. Both pre-cultures and main cultures were supplemented with 0.025% (w/v) natural L-lysine (“light” lysine, Lys0, K0, Sigma Aldrich). The expression of *hipA* was induced with 0.2% (w/v) arabinose at OD_{600nm} of ≈0.4. After 3 hours of *hipA* expression, cultures were treated with 0.4% glucose and 100 µg/ml ampicillin for around 22 hours. To induce resuscitation, cultures were first quickly filtered using pre-warmed 1 l Corning filter system (0.22 µm pore size) to remove ampicillin, Lys0 and dead cells. Immediately after, cells were

quickly recovered in pre-warmed medium supplemented with 25 µg/ml chloramphenicol, 50 µg/ml kanamycin, 0.4% glucose, 0.025% Lys8 and 2 mM β-D-1-thiogalactopyranoside (IPTG) for the induction of the P_{lac}*::hipB* fusion. Cells were harvested at intermittent time intervals (10min - 30h) by centrifugation at 4 ˚C. A time point before filtering and Lys8 pulse (0h) was harvested as a control.

Cell lysis and sample preparation

Collected cell pellets were lyzed in a lysis buffer (40 mg/ml SDS, 100 mM Tris-HCl pH 8.6, 10 mM EDTA and Complete protease inhibitors (Roche)) and sonicated 3 times for 30 s at 40% amplitude. The cellular debris was pelleted by centrifugation at 15,000 g for 30 min at room temperature and proteins were precipitated from the supernatant with chloroform and methanol. Protein pellets were dissolved in a denaturation buffer (6 M urea, 2 M thiourea and 10 mM Tris pH 8.0). Protein concentration was determined using standard Bradford assay (Bio-Rad). A 10 µg protein aliquot from each time point was reduced using 1 mM dithiotreitol for one hour and alkylated with 5.5 mM iodoacetamide for additional hour. Proteins were pre-digested with endoproteinase Lys-C (1:100 w/w) for 3 hours, then diluted with 4 volumes of 20 mM ammonium bicarbonate, pH 8.0 and digested overnight with Lys-C (1:100 w/w) at room temperature. The reaction was stopped by lowering pH to 2 with trifluoroacetic acid. Peptides were purified via stage tips (Rappsilber et al., 2007) as described previously (Semanjski et al., 2018). Briefly, before each LC-MS/MS measurement, samples were de- salted and purified on reversed-phase C18 stage tips (Empore), in-house prepared, previously activated with methanol and equilibrated with solvent A*. Up to 10 µg of peptides were loaded onto the membrane, washed with solvent A and then eluted with 50 µl of solvent B [80% (v/v) acetonitrile and 0.1% (v/v) formic acid] and concentrated by vacuum centrifugation. The sample volume was adjusted with solvent A and final 10% (v/v) of solvent A*.

LC-MS/MS measurement

Samples from each time point were separated by the EASY-nLC 1200 system (Thermo Scientific). Peptide separation was performed by reversed-phase chromatography on the in-house packed analytical column (20 cm × 75 µm, 1.9 µm ReproSil-Pur C18-AQ particles (Dr. Maisch)). Peptides were loaded onto the column at a flow rate of 700 nl/min of solvent A (0.1% (v/v) formic acid) and a constant temperature of 40 °C under maximum back-pressure of 850 bar. Peptides were eluted using 116 min segmented gradient of 10 – 50% solvent B (80% (v/v) acetonitrile, 0.1% (v/v) formic acid) at a flow rate of 200 nl/min. Peptides were infused directly from the column tip into the on-line coupled Q Exactive HF mass spectrometer (Thermo Scientific) using nanoelectrospray ion source (Thermo Scientific) at a voltage of 2.3 kV and a temperature of 275 ˚C. Positively charged peptides were analyzed in a data-dependent acquisition mode, in which one full scan and subsequent MS/MS scans of 12 (Top12 method) most abundant precursors (isolation window of 1.4 m/z) were recorded in a mass range from 300 to 1,650 m/z. To prevent repeated fragmentation, the masses of sequenced precursors were dynamically excluded for 30 s. Only precursors with assigned charge states ≥ 2 and ≤ 5 were considered for fragmentation selection. Full scans were acquired with a resolution of 60,000 at m/z 200, the maximum injection time of 25 ms and the automatic gain control (AGC) target value of 3×10^6 charges. The higher energy collisional dissociation (HCD) fragmentation was achieved at normalized collision energy of 27% and intensity threshold of 1×10^5. MS/MS spectra were acquired with the resolution of 30,000, the maximum injection time of 45 ms and the AGC target value of 1×10^5 charges.

MS data processing and analysis

Acquired raw data was processed with MaxQuant software (version 1.5.2.8) (Cox and Mann, 2008) using the default settings if not stated otherwise. Raw files of particular experiments were processed separately.

The built-in Andromeda search engines searched MS/MS spectra against fragment masses of peptides derived from an *E. coli* K12 reference proteome (taxonomy ID 83333) containing 4,324 entries (UniProt, release 2017/12) and a list of 245 common contaminants. The minimum required peptide length was set to 7 amino acids with the maximum of two missed cleavage sites allowed for endoproteinase Lys-C. For a protein to be quantified, two occurrences of the protein H/L ratio were required per time point (the multiplicity was set to two with Lys8 specified as the heavy label). Carbamidomethylation of cysteine was set as a fixed modification, and protein N-terminal acetylation and methionine oxidation as variable modifications. Precursor ion mass tolerance was set to 20 ppm in the first search and to 4.5 ppm and in the main search. Peptide and protein identifications were filtered using a target-decoy approach with a an estimated false discovery rate (FDR) of less than 1.3% at protein and less than 0.4% at peptide level(Elias and Gygi, 2007). Proteins identified by the same set of peptides were combined into a single protein group. For protein quantification, at least 2 peptide ratio counts were required.

Data analysis was performed using Microsoft Excel and Perseus software (version 1.5.6.0)(Tyanova et al., 2016). Non-normalized protein H/L ratios from proteingroup.txt were used for protein quantification. All contaminants, reversed hits and proteins identified only by modification were removed. To simplify the data, the data sets from three biological replicate measurements were combined as a union, in which protein H/L ratios in each of the time points were kept if measured only in one replicate (Class I), a mean was calculated if measured in two (Class II) or in three replicates (Class III). To reduce the number of data points and missing values, time points were pooled into time bins. For that, the median protein H/L ratio of respective time points was calculated and assigned to a specific time bin. Proteins were then ranked based on their H/L ratio within each time bin and displayed in a heatmap-like representation sorted by the maximal H/L ratio across time bins. Gene-annotation and KEGG enrichment analysis was performed using DAVID tool (version 6.8) with default parameters and the background of all quantified proteins in particular experiment (Huang et al., 2008).

Temporal analysis of label incorportion

MaxQuant processed data were imported in the R environment (R Core Team, 2018) to perform a time series analysis. The heavy label incorporation was calculated by dividing the heavy label intensity by the total (heavy plus light) intensity for each protein. Reverse hits, potential contaminants and proteins only identified by sites were filtered out. The median of three replicates was computed per time points. Proteins with missing values were discarded from further analysis. The Euclidean distance between proteins was computed and used to generate the hierarchical clustering via the Ward's minimum distance using the stats R package. Time period resolution was achieved with minimal overlap when using eight cluster groups (k = 8). The resulting heatmap was drawn using the gplots R package (Warnes et al., 2019), while cluster protein profiles over time were generated using the ggplot2 R package (Wickham, 2016). For each cluster, the time needed to reach 50% heavy label incorporation was inferred by intersecting the 50% incorporation with the smoothed conditional mean. The list of proteins belonging to each cluster were imported into Perseus software suite (version 1.6.5.0) (Tyanova et al., 2016). The proteins were functionally annotated with Gene Ontology, KEGG, Pfam, GSEA, UniProt keywords, Corum, Interpro, Reactome and EC functional resources. Each cluster was tested for function categories over- or under-representation using a fisher exact test (FDR ≤ 0.1).

Reactive web application for data browsing

To allow the scientific community to browse our datasets, we developed a Shiny application coded entirely in the R programming language (Chang et al., 2019). Our application, called PCTsee, allows user to load different datasets, which are available through a drop down widget. It is then possible to select gene name or protein ID of interest in order to display their abundance value. Whereby the abundance values have

been computed by the MaxQuant software during LC-MS/MS data processing (e.g. intensity, ratio). The user selection will result in a protein abundance profile plot, as well as a table containing some information about the selected protein (e.g. protein names, sequence coverage). Users can interact further with the displayed plot to zoom, rescale or remove samples due to the plotly R package (Sievert, 2018). PCTsee application is available at the following address: https://pctsee.pct.uni-tuebingen.de.

GO_term enrichment

Gene onhtology analysis of the proteins actively synthesized during resuscitation was perform with the online software DAVID (https://david.ncifcrf.gov/tools.jsp). Enrichment was performed comparing the gene names quantified proteins against the ones of identified proteins. DAVID was used with its preset with: similarity overlap 3 and threshold 0.5; initial and final group membership 3 and multiple linkage 0.5; enrichment thresohold at EASE 1.

Calculation of protein turnover rates

Protein turnover rate (*k*) was calculated by linear regression of natural logarithm of protein SILAC H/L ratio over time as described previously(Schwanhäusser et al., 2011) using equation independent of the growth rate:

$$k = \frac{\sum_{i=1}^{m} log_e(r_{t_i} + 1)t_i}{\sum_{i=1}^{m} t_i^2}$$

Where *m* is the number of time points (t_i) and r_{t_i} is protein H/L ratio measured in a time point t_i. The half-life of a protein ($T_{1/2}$) was calculated by dividing the natural logarithm with the turnover rate *k*:

$$T_{1/2} = \frac{log_e 2}{k}$$

Protein H/L ratios derived from a union of three replicates were used for the calculation and only proteins with H/L ratio measured in > 4 time points were considered. As a quality check of linear regression, the coefficient of determination (R^2) was required to be > 0.70 to ensure good curve fitting and reliable turnover rate estimation. All proteins with determined protein turnover rates are reported in the **Supplementary Table S5**.

The mass spectrometry proteomics data have been deposited to the ProteomeXchange Consortium via the PRIDE (Vizcaíno et al., 2016) partner repository with the dataset identifier PXD018153. All other data needed to evaluate the conclusions in this paper are present in the paper or the Supplementary Materials.

Figure legends

Figure 1. Persister cells synthesize proteins involved in essential physiological processes. (A) Transcription of plasmid-encoded *hipA* (pBAD33*::hipA*) was induced in *E. coli* K-12 strain MG1655 at an optical density OD_{600nm} of 0.4 for 3 hours, followed by ampicillin treatment and addition of glucose to repress further *hipA* transcription. Approx. 20 hours after *hipA* induction, the culture was sampled at 17 time points. Proteins were digested with endoproteinase Lys-C and measured by LC-MS/MS. The growth curve is representative of three biological replicates. **(B)** Incorporation of Lys8 into proteins across 17 time points calculated from the measured protein H/L ratios. The box plots are representative of 3 biological replicates. **(C)** Heat map of all quantified proteins color-coded based on their H/L ratio ranking within each time bin. Missing values are colored in grey. KEGG pathway enrichment analysis of quanified proteins in the 25th percentile (Top 25%, red), 25th – 50th percentile (pink), 50th – 75th percentile (light blue) and 75th percentile (Bottom 25%, blue) across all time bins. The number of enriched proteins in each category

is indicated outside the bars. **(D-F)** Label incorporation curves of selected examples of enzymes involved in protein degradation, translation and folding (chaperones).

Figure 2. Ribosome-associated proteins RaiA and Sra show elevated synthesis levels in persisting cells and a role during antibiotic tolerance. (A) All detected ribosomal proteins had comparable label incorporation rates. The synthesis rate of the hibernation factor RaiA was elevated and similar to ribosomal proteins, whereas the synthesis rate of the ribosome-associated protein Sra was markedly higher than that of the ribosomal proteins. Most of the ribosome-associated hibernation factors (e.g. EttA, ElaB, YqjD) showed very low synthesis levels. **(B)** Estimates of the amounts of newly synthesized proteins based on intensity-based absolute quantification (IBAQ) (Schwanhäusser et al., 2011) in the heavy SILAC channel. The amount of newly synthesized RaiA and Sra proteins was about 100 times higher than all ribosomal proteins combined. Depicted are the median values of three biological replicates. **(C)** WT strains ectopically expressing HipA were more viable compared to the same strain bearing the empty vector. Two deletion strains (*Δsra* and *ΔraiA*) expressing *hipA* showed a strong decrease in CFU, indicating potential role of Sra and RaiA in the antibiotic-tolerance mechanism. Two-way ANOVA showed difference in survival between the two mutants and the WT strains, but also between *sra* and *raiA* mutants (at 120 min), pointing to potentially different functions of the two proteins in the persistence mechanism.

Figure 3. Resuscitating cells restore metabolic activity and translation machinery (A) Transcription of *hipA* was induced and repressed as described in the Legend to Figure 1. To trigger resuscitation, a culture sample was filtered and cells transferred into fresh medium containing IPTG to induce expression of *hipB* (p_{lac}*::hipB*) and "heavy" lysine (Lys8) for pulse-labeling. Cells were harvested at 21 time points thereafter. The growth curve is representative of three biological replicates. **(B)** Incorporation of Lys8 into proteins across 21 time points calculated from the measured protein H/L ratios. The box plots are representative

of 3 biological replicates. **(C)** Heat map of all quantified proteins color-coded based on their H/L ratio ranking within each time bin. Missing values are colored in grey. KEGG enrichment analysis of proteins in the 25th percentile (Top 25%, red), 25th – 50th percentile (pink), 50th – 75th percentile (light blue) and 75th percentile (Bottom 25%, blue) across all time bins was performed with DAVID software against the background of all quantified proteins. The number of enriched proteins in each category is indicated outside the bars. **(D-F)** Label incorporation curves of selected examples of enzymes involved in protein and folding (chaperones), translation and degradation.

Figure 4. Ribosomal proteins, but also hibernation factors are heavily synthesized in resuscitating cells. **(A)** Label incorporation rates of ribosomal proteins and selected hibernation factors during resuscitation. All ribosomal proteins, except L31-B and L36-2, showed concerted synthesis levels (dotted red trace). The hibernation factor HflX was induced at the onset of resuscitation. Remarkably, ribosome-associated proteins RaiA and Sra were also heavily synthesized. **(B)** Estimates of the amounts of newly synthesized proteins based on IBAQ in the heavy SILAC channel. In contrast to persistence, the amounts of newly synthesized ribosomal proteins are similar to the amounts of newly synthesized RaiA and Sra proteins. The estimated amount of HflX is about 100 times lower.

Supplementary Material

Supplementary Figure 1. Measurement of newly synthesized proteins in persisting *E. coli* cells. (A) OD_{600} measurement of the *E. coli* culture after induction of ectopic hipA expression compared to the empty vector. **(B)** CFU measurement of the hipA-expressing *E. coli* culture at several points before and after ampicillin addition. *E. coli* cell containing empty vector were used as control. **(C)** Biochemical and mass

spectrometry workflow employed in our study. **(D)** Lys8 label incorporation monitored by increasing number of quantified proteins over 24 hours. Quantified proteins were detected in both "light" ("L") and "heavy" ("H") form, which enabled calculation of their H/L ration (relative quantification). **(E)** Correlation plot of two biological replicates demonstrates high reproducibility. (F) Estimated half-lifes of newly synthesized proteins during persistence.

Supplementary Figure 2. Measurement of newly synthesized proteins in resuscitating *E. coli* cells. (A) OD_{600} measurements of *hipB*-induced and -uninduced ("no filter") cultures confirm that resuscitation was driven by ectopic *hipB* expression. In the absence of hipB expression the OD_{600} remained constant for at least 30 hours, demonstrating that no spontaneous resuscitation or development of resistance occurred during this time period. **(B)** Lys8 label incorporation monitored by increasing number of quantified proteins over 30 hours. Note that after eight hours cell entered the exponential growth, which led to exponential increase of the heavy signal intensity. After this time point numerous proteins are predominantly present in their heavy form and their H/L ratio cannot be calculated, which leads to an apparent "decrease" of the quantified proteins. **(C)** Correlation plot of two biological replicates demonstrates high reproducibility. **(D)** Abundance traces of ribosomal proteins L31 (rpmE) and L36 (rpmJ), and their paralogs L31 type B (ykgM) and L36 2 (ykgO) point to a rearrangement of the large ribosomal unit at the entrance to stationary phase.

Supplementary Figure 3. Map of top 25 quantified proteins with highest incorporation of Ly8 in each time bin during resuscitation. Different functional descriptions are color coded according to the legend. Boxes around individual proteins are coded based on the style of the line and indicate the confidence of protein quantification per time bin according to the following classification system: protein is quantified

in > 67% of the time points in 3 replicates (Class I), protein is quantified in < 67% and > 33% of the time points in 3 replicates (Class II), protein is quantified in < 33% of the time points in 3 replicates (Class III).

Supplementary Figure 4. Clustering of label incorporation profiles allows reconstruction of time-dependant cell metabolism during resuscitation. Heavy label incorporation was used to cluster proteins across the resuscitation time scale. Among the eight clusters represented, clusters 8, 4 and 1 belong to the early synthesized proteins; clusters 5, 3 and 2 belong to the medium proteins; and clusters 6 and 7 belong to the late proteins. The smoothed conditional means is represented as a dashed curve within each cluster. For each cluster the time at 50% incorporation is determined based on the intersection with smoothed means. The top significantly over-represented functional category for each cluster (FDR ≤ 0.05) are plotted on the right panels.

Acknowledgements

The authors thank Christiane Wolz and Karl Forchhammer for useful discussions and comments on the manuscript. B.M. was supported by grants from the Deutsche Forschungsgemeinschaft (German Research Foundation Cluster of Excellence EXC 2124, SFB 766, FOR 2816, TRR 261) and the German–Israeli Foundation (I-1464–416.13/2018). K.G. was supported by a grant from the Danish National Research Foundation (grant identifier DNRF120) and the Novo Nordisk Foundation.

References

Amato, S.M., Fazen, C.H., Henry, T.C., Mok, W.W.K., Orman, M.A., Sandvik, E.L., Volzing, K.G., and Brynildsen, M.P. (2014). The role of metabolism in bacterial persistence. Frontiers in Microbiology *5*, 70.

Baba, T., Ara, T., Hasegawa, M., Takai, Y., Okumura, Y., Baba, M., Datsenko, K.A., Tomita, M., Wanner, B.L., and Mori, H. (2006). Construction of Escherichia coli K-12 in-frame, single-gene knockout mutants: the Keio collection. Molecular systems biology *2*, 2006 0008.

Balaban, N.Q. (2011). Persistence: mechanisms for triggering and enhancing phenotypic variability. Current Opinion in Genetics & Development *21*, 768-775.

Balaban, N.Q., Helaine, S., Lewis, K., Ackermann, M., Aldridge, B., Andersson, D.I., Brynildsen, M.P., Bumann, D., Camilli, A., Collins, J.J*., et al.* (2019). Definitions and guidelines for research on antibiotic persistence. Nature reviews Microbiology *17*, 441-448.

Balaban, N.Q., Merrin, J., Chait, R., Kowalik, L., and Leibler, S. (2004). Bacterial Persistence as a Phenotypic Switch. Science *305*, 1622-1625.

Battesti, A., Majdalani, N., and Gottesman, S. (2011). The RpoS-mediated general stress response in Escherichia coli. Annual review of microbiology *65*, 189-213.

Brauner, A., Fridman, O., Gefen, O., and Balaban, N.Q. (2016). Distinguishing between resistance, tolerance and persistence to antibiotic treatment. Nature Reviews Microbiology *14*, 320.

Canas-Duarte, S.J., Restrepo, S., and Pedraza, J.M. (2014). Novel protocol for persister cells isolation. PloS one *9*, e88660.

Cañas-Duarte, S.J., Restrepo, S., and Pedraza, J.M. (2014). Novel Protocol for Persister Cells Isolation. PLOS ONE *9*, e88660.

Chua, S.L., Yam, J.K., Hao, P., Adav, S.S., Salido, M.M., Liu, Y., Givskov, M., Sze, S.K., Tolker-Nielsen, T., and Yang, L. (2016). Selective labelling and eradication of antibiotic-tolerant bacterial populations in Pseudomonas aeruginosa biofilms. Nat Commun *7*, 10750.

Cox, J., and Mann, M. (2008). MaxQuant enables high peptide identification rates, individualized p.p.b.-range mass accuracies and proteome-wide protein quantification. Nature Biotechnology *26*, 1367.

Denby, K.J., Iwig, J., Bisson, C., Westwood, J., Rolfe, M.D., Sedelnikova, S.E., Higgins, K., Maroney, M.J., Baker, P.J., Chivers, P.T*., et al.* (2016). The mechanism of a formaldehyde-sensing transcriptional regulator. Scientific Reports *6*, 38879.

Dieterich, D.C., Lee, J.J., Link, A.J., Graumann, J., Tirrell, D.A., and Schuman, E.M. (2007). Labeling, detection and identification of newly synthesized proteomes with bioorthogonal non-canonical amino-acid tagging. Nature Protocols *2*, 532.

Doherty, M.K., Hammond, D.E., Clague, M.J., Gaskell, S.J., and Beynon, R.J. (2009). Turnover of the Human Proteome: Determination of Protein Intracellular Stability by Dynamic SILAC. Journal of Proteome Research *8*, 104-112.

Elias, J.E., and Gygi, S.P. (2007). Target-decoy search strategy for increased confidence in large-scale protein identifications by mass spectrometry. Nature Methods *4*, 207.

Germain, E., Castro-Roa, D., Zenkin, N., and Gerdes, K. (2013). Molecular Mechanism of Bacterial Persistence by HipA. Molecular Cell *52*, 248-254.

Gohara, D.W., and Yap, M.F. (2018). Survival of the drowsiest: the hibernating 100S ribosome in bacterial stress management. Curr Genet *64*, 753-760.

Gotfredsen, M., and Gerdes, K. (1998). The Escherichia coli relBE genes belong to a new toxin–antitoxin gene family. Molecular Microbiology *29*, 1065-1076.

Gottesman, S., Roche, E., Zhou, Y., and Sauer, R.T. (1998). The ClpXP and ClpAP proteases degrade proteins with carboxy-terminal peptide tails added by the SsrA-tagging system. Genes Dev *12*, 1338-1347.

Guyer, M., Reed, R., Steitz, J., and Low, K. (1981). Identification of a sex-factor-affinity site in E. coli as γδ. Paper presented at: Cold Spring Harbor symposia on quantitative biology (Cold Spring Harbor Laboratory Press).

Guzman, L.M., Belin, D., Carson, M.J., and Beckwith, J. (1995). Tight regulation, modulation, and high-level expression by vectors containing the arabinose PBAD promoter. Journal of Bacteriology *177*, 4121-4130.

Hansen, S., Lewis, K., and Vulić, M. (2008). Role of Global Regulators and Nucleotide Metabolism in Antibiotic Tolerance in Escherichia coli. Antimicrobial Agents and Chemotherapy *52*, 2718-2726.

Harms, A., Maisonneuve, E., and Gerdes, K. (2016). Mechanisms of bacterial persistence during stress and antibiotic exposure. Science *354*.

Helaine, S., Cheverton, A.M., Watson, K.G., Faure, L.M., Matthews, S.A., and Holden, D.W. (2014). Internalization of Salmonella by Macrophages Induces Formation of Nonreplicating Persisters. Science *343*, 204-208.

Huang, D.W., Sherman, B.T., and Lempicki, R.A. (2008). Systematic and integrative analysis of large gene lists using DAVID bioinformatics resources. Nature Protocols *4*, 44.

Jõers, A., Kaldalu, N., and Tenson, T. (2010). The Frequency of Persisters in Escherichia coli Reflects the Kinetics of Awakening from Dormancy. Journal of Bacteriology *192*, 3379-3384.

Keren, I., Shah, D., Spoering, A., Kaldalu, N., and Lewis, K. (2004). Specialized Persister Cells and the Mechanism of Multidrug Tolerance in Escherichia coli. Journal of Bacteriology *186*, 8172-8180.

Lewis, K. (2010). Persister Cells. Annual Review of Microbiology *64*, 357-372.

Lilleorg, S., Reier, K., Pulk, A., Liiv, A., Tammsalu, T., Peil, L., Cate, J.H.D., and Remme, J. (2019). Bacterial ribosome heterogeneity: Changes in ribosomal protein composition during transition into stationary growth phase. Biochimie *156*, 169-180.

Maciąg, A., Peano, C., Pietrelli, A., Egli, T., De Bellis, G., and Landini, P. (2011). In vitro transcription profiling of the σ S subunit of bacterial RNA polymerase: re-definition of the σ S regulon and identification of σ S -specific promoter sequence elements. Nucleic Acids Research *39*, 5338-5355.

Miura, K., Tomioka, Y., Hoshi, Y., Suzuki, H., Yonezawa, M., Hishinuma, T., and Mizugaki, M. (1997). The effects of unsaturated fatty acids, oxidizing agents and Michael reaction acceptors on the induction of N-ethylmaleimide reductase in Escherichia coli: possible application for drug design of chemoprotectors. Methods Find Exp Clin Pharmacol *19*, 147-151.

Page, R., and Peti, W. (2016). Toxin-antitoxin systems in bacterial growth arrest and persistence. Nature Chemical Biology *12*, 208.

Prossliner, T., Skovbo Winther, K., Sorensen, M.A., and Gerdes, K. (2018). Ribosome Hibernation. Annu Rev Genet *52*, 321-348.

Pu, Y., Zhao, Z., Li, Y., Zou, J., Ma, Q., Zhao, Y., Ke, Y., Zhu, Y., Chen, H., Baker, M.A.B.*, et al.* (2016). Enhanced Efflux Activity Facilitates Drug Tolerance in Dormant Bacterial Cells. Mol Cell *62*, 284-294.

Radzikowski, J.L., Schramke, H., and Heinemann, M. (2017). Bacterial persistence from a system-level perspective. Curr Opin Biotechnol *46*, 98-105.

Rappsilber, J., Mann, M., and Ishihama, Y. (2007). Protocol for micro-purification, enrichment, pre-fractionation and storage of peptides for proteomics using StageTips. Nature Protocols *2*, 1896.

Ringquist, S., Shinedling, S., Barrick, D., Green, L., Binkley, J., Stormo, G.D., and Gold, L. (1992). Translation initiation in Escherichia coli: sequences within the ribosome-binding site. Molecular Microbiology *6*, 1219-1229.

Rowe, S.E., Conlon, B.P., Keren, I., and Lewis, K. (2016). Persisters: Methods for Isolation and Identifying Contributing Factors--A Review. Methods in molecular biology *1333*, 17-28.

Schumacher, M.A., Balani, P., Min, J., Chinnam, N.B., Hansen, S., Vulić, M., Lewis, K., and Brennan, R.G. (2015). HipBA–promoter structures reveal the basis of heritable multidrug tolerance. Nature *524*, 59.

Schwanhäusser, B., Busse, D., Li, N., Dittmar, G., Schuchhardt, J., Wolf, J., Chen, W., and Selbach, M. (2011). Global quantification of mammalian gene expression control. Nature *473*, 337.

Semanjski, M., Germain, E., Bratl, K., Kiessling, A., Gerdes, K., and Macek, B. (2018). The kinases HipA and HipA7 phosphorylate different substrate pools in Escherichia coli to promote multidrug tolerance. Sci Signal *11*.

Shah, D., Zhang, Z., Khodursky, A.B., Kaldalu, N., Kurg, K., and Lewis, K. (2006). Persisters: a distinct physiological state of E. coli. BMC Microbiology *6*, 53.

Spanka, D.T., Konzer, A., Edelmann, D., and Berghoff, B.A. (2019). High-Throughput Proteomics Identifies Proteins With Importance to Postantibiotic Recovery in Depolarized Persister Cells. Front Microbiol *10*, 378.

Spat, P., Klotz, A., Rexroth, S., Macek, B., and Forchhammer, K. (2018). Chlorosis as a Developmental Program in Cyanobacteria: The Proteomic Fundament for Survival and Awakening. Mol Cell Proteomics *17*, 1650-1669.

Sulaiman, J.E., Hao, C., and Lam, H. (2018). Specific Enrichment and Proteomics Analysis of Escherichia coli Persisters from Rifampin Pretreatment. J Proteome Res *17*, 3984-3996.

Tyanova, S., Temu, T., Sinitcyn, P., Carlson, A., Hein, M.Y., Geiger, T., Mann, M., and Cox, J. (2016). The Perseus computational platform for comprehensive analysis of (prote)omics data. Nature Methods *13*, 731.

Umezawa, Y., Shimada, T., Kori, A., Yamada, K., and Ishihama, A. (2008). The Uncharacterized Transcription Factor YdhM Is the Regulator of the nemA Gene, Encoding N-Ethylmaleimide Reductase. Journal of Bacteriology *190*, 5890-5897.

Van den Bergh, B., Fauvart, M., and Michiels, J. (2017). Formation, physiology, ecology, evolution and clinical importance of bacterial persisters. FEMS Microbiology Reviews *41*, 219-251.

Varik, V., Oliveira, S.R.A., Hauryliuk, V., and Tenson, T. (2016). Composition of the outgrowth medium modulates wake-up kinetics and ampicillin sensitivity of stringent and relaxed Escherichia coli. Scientific Reports *6*, 22308.

Ventola, C.L. (2015). The Antibiotic Resistance Crisis: Part 1: Causes and Threats. Pharmacy and Therapeutics *40*, 277-283.

Vizcaíno, J.A., Csordas, A., del-Toro, N., Dianes, J.A., Griss, J., Lavidas, I., Mayer, G., Perez-Riverol, Y., Reisinger, F., Ternent, T.*, et al.* (2016). 2016 update of the PRIDE database and its related tools. Nucleic Acids Research *44*, D447-D456.

Yoshida, H., and Wada, A. (2014). The 100S ribosome: ribosomal hibernation induced by stress. Wiley Interdiscip Rev RNA *5*, 723-732.

Zhang, Y., Mandava, C.S., Cao, W., Li, X., Zhang, D., Li, N., Zhang, Y., Zhang, X., Qin, Y., Mi, K.*, et al.* (2015). HflX is a ribosome-splitting factor rescuing stalled ribosomes under stress conditions. Nature structural & molecular biology *22*, 906-913.

Figure 1

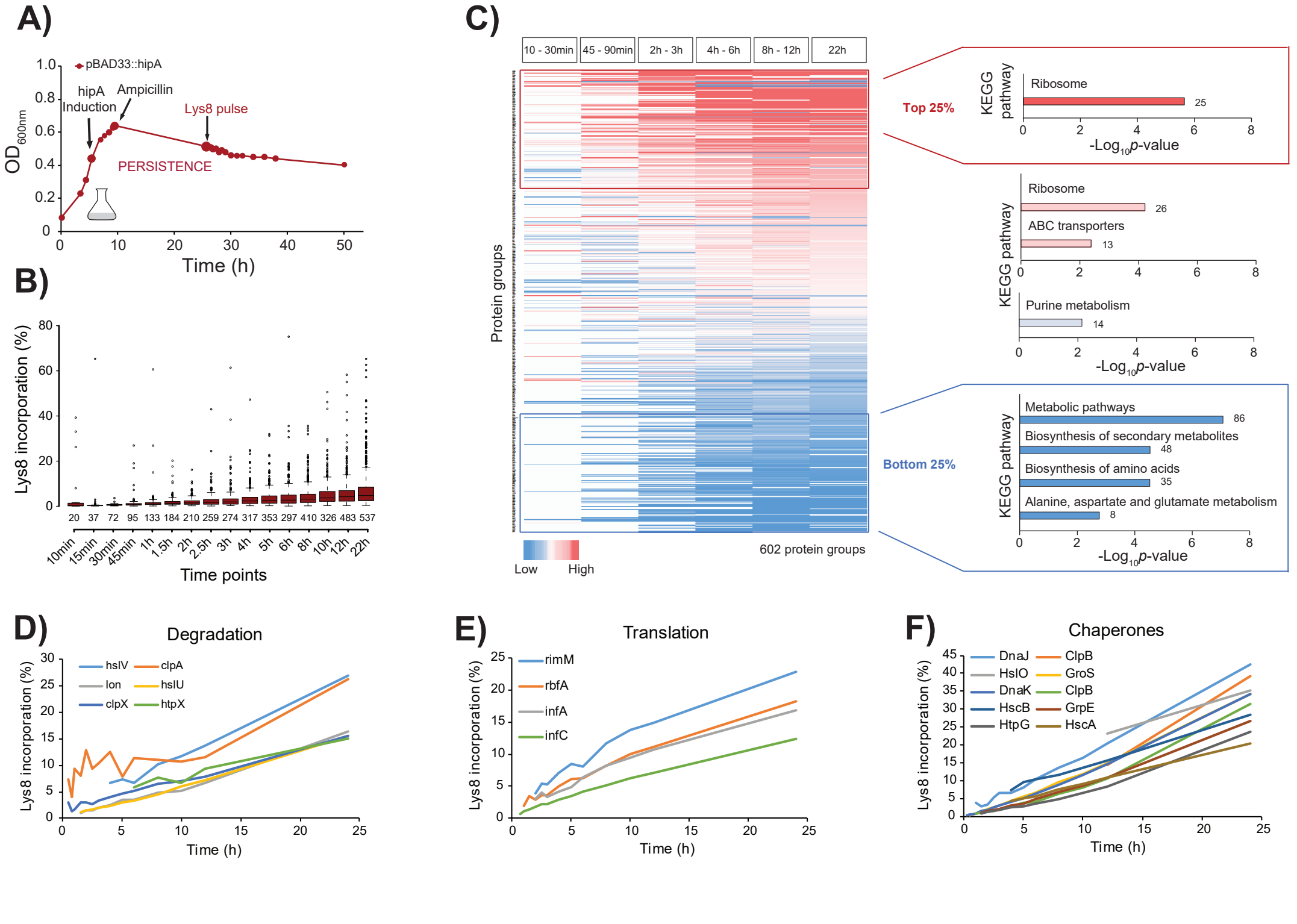
A)
pBAD33::hipA
hipA Induction
Ampicillin
Lys8 pulse
PERSISTENCE
OD600nm
Time (h)
B)
Lys8 incorporation (%)
20 37 72 95 133 184 210 259 274 317 353 297 410 326 483 537
10min 15min 30min 45min 1h 1.5h 2h 2.5h 3h 4h 5h 6h 8h 10h 12h 22h
Time points
C)
10 - 30min
45 - 90min
2h - 3h
4h - 6h
8h - 12h
22h
Protein groups
602 protein groups
Low
High
Top 25%
KEGG pathway
Ribosome
25
-Log10p-value
Ribosome
26
ABC transporters
13
Purine metabolism
14
Bottom 25%
Metabolic pathways
86
Biosynthesis of secondary metabolites
48
Biosynthesis of amino acids
35
Alanine, aspartate and glutamate metabolism
8
D)
Degradation
hslV
clpA
lon
hslU
clpX
htpX
Lys8 incorporation (%)
Time (h)
E)
Translation
rimM
rbfA
infA
infC
Lys8 incorporation (%)
Time (h)
F)
Chaperones
DnaJ
ClpB
HslO
GroS
DnaK
ClpB
HscB
GrpE
HtpG
HscA
Lys8 incorporation (%)
Time (h)

Figure 2

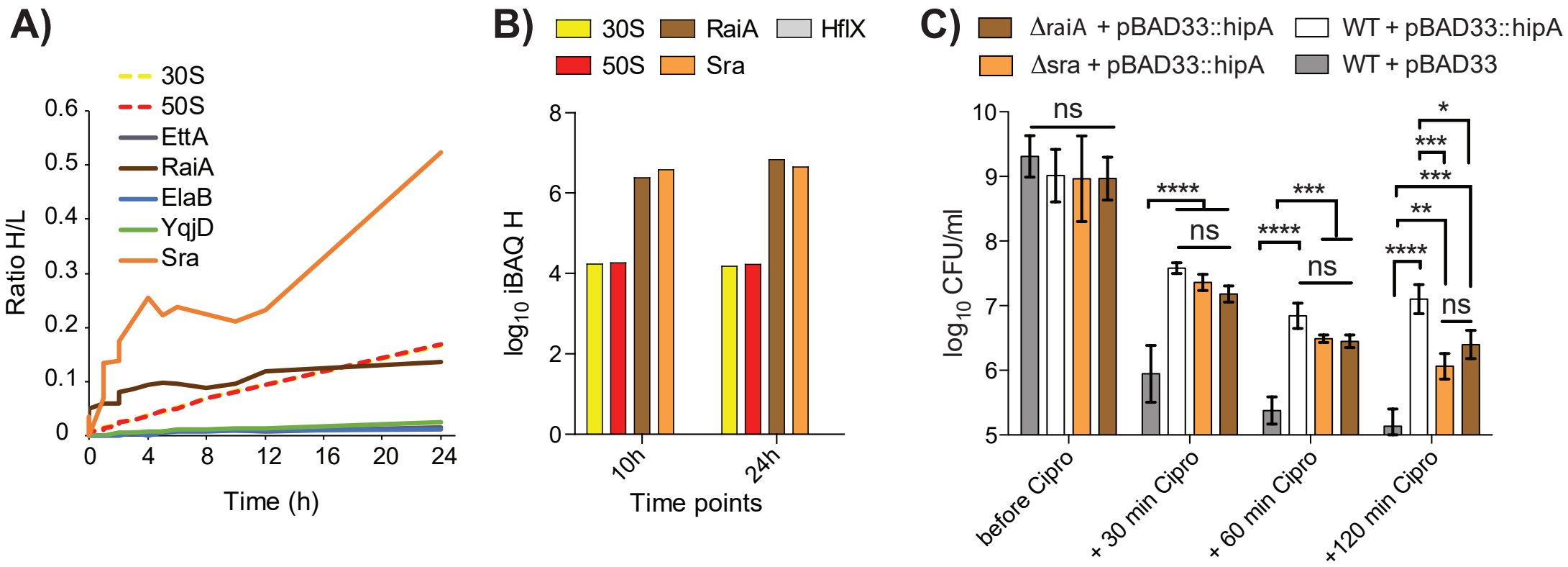
A)
30S
50S
EttA
RaiA
ElaB
YqjD
Sra
Ratio H/L
0.6
0.5
0.4
0.3
0.2
0.1
0
0
4
8
12
16
20
24
Time (h)
B)
30S
RaiA
HflX
50S
Sra
log10 iBAQ H
8
6
4
2
0
10h
24h
Time points
C)
ΔraiA + pBAD33::hipA
WT + pBAD33::hipA
Δsra + pBAD33::hipA
WT + pBAD33
log10 CFU/ml
10
9
8
7
6
5
ns
****
ns
***
****
ns
*
***
**
****
ns
before Cipro
+ 30 min Cipro
+ 60 min Cipro
+120 min Cipro

Figure 3

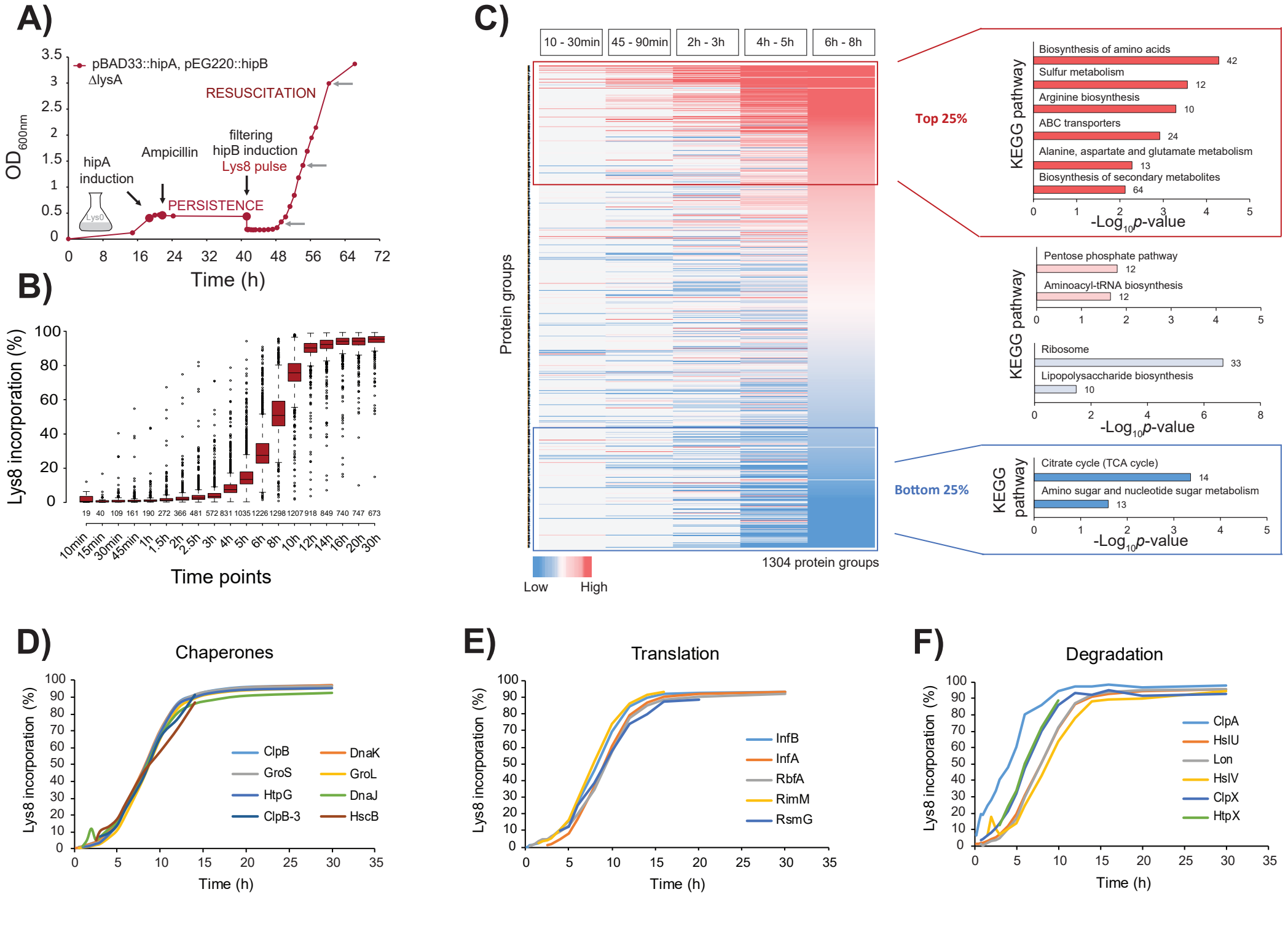
A)
pBAD33::hipA, pEG220::hipB
ΔlysA
RESUSCITATION
filtering
hipB induction
Lys8 pulse
Ampicillin
hipA
induction
PERSISTENCE
Lys0
OD600nm
Time (h)
B)
Lys8 incorporation (%)
19 40 109 161 190 272 366 481 572 831 1035 1226 1298 1207 918 849 740 747 673
10min 15min 30min 45min 1h 1.5h 2h 2.5h 3h 4h 5h 6h 8h 10h 12h 14h 16h 20h 30h
Time points
C)
10 - 30min
45 - 90min
2h - 3h
4h - 5h
6h - 8h
Protein groups
1304 protein groups
Low
High
Top 25%
KEGG pathway
Biosynthesis of amino acids 42
Sulfur metabolism 12
Arginine biosynthesis 10
ABC transporters 24
Alanine, aspartate and glutamate metabolism 13
Biosynthesis of secondary metabolites 64
-Log10p-value
Pentose phosphate pathway 12
Aminoacyl-tRNA biosynthesis 12
Ribosome 33
Lipopolysaccharide biosynthesis 10
Bottom 25%
Citrate cycle (TCA cycle) 14
Amino sugar and nucleotide sugar metabolism 13
D)
Chaperones
ClpB
GroS
HtpG
ClpB-3
DnaK
GroL
DnaJ
HscB
E)
Translation
InfB
InfA
RbfA
RimM
RsmG
F)
Degradation
ClpA
HslU
Lon
HslV
ClpX
HtpX
Time (h)

Figure 4

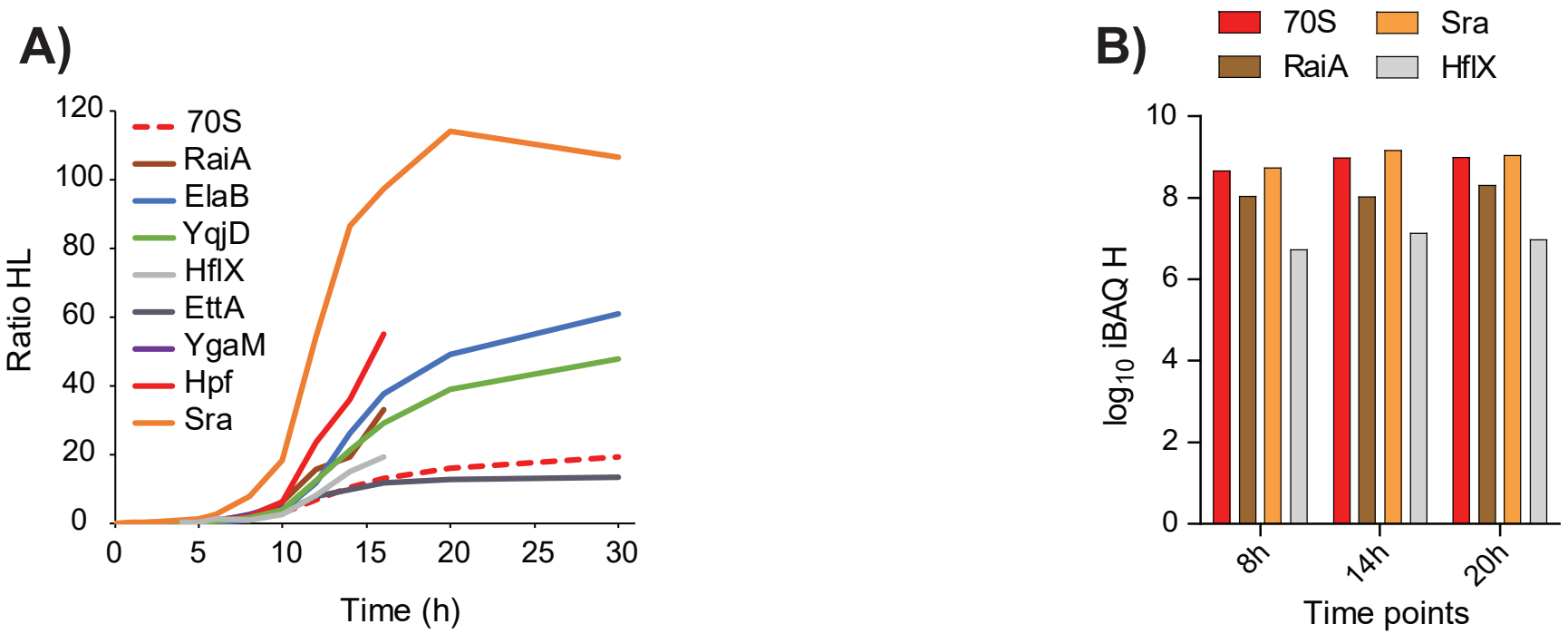
A)
Ratio HL
120
100
80
60
40
20
0
70S
RaiA
ElaB
YqjD
HflX
EttA
YgaM
Hpf
Sra
0
5
10
15
20
25
30
Time (h)
B)
70S
Sra
RaiA
HflX
log10 iBAQ H
10
8
6
4
2
0
8h
14h
20h
Time points

Suppl. Figure 1

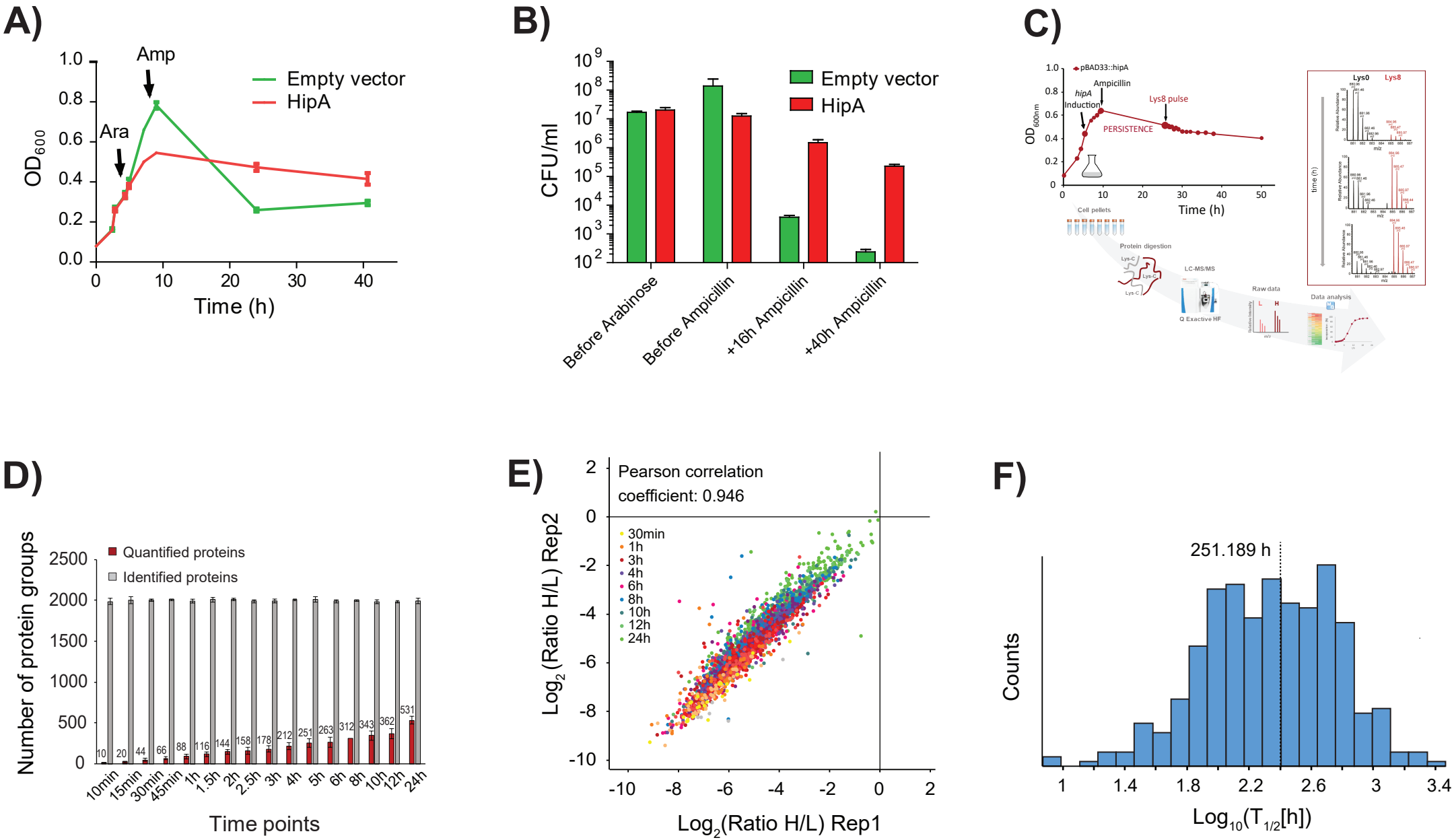

Suppl. Figure 2

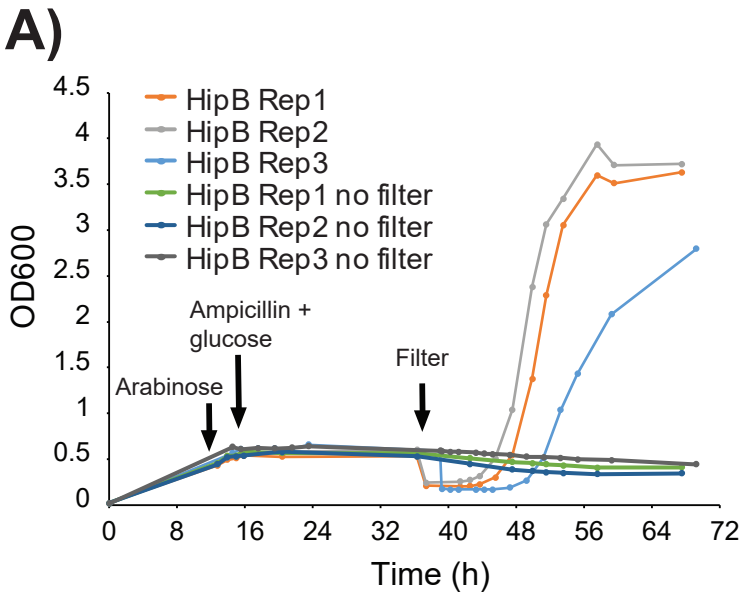

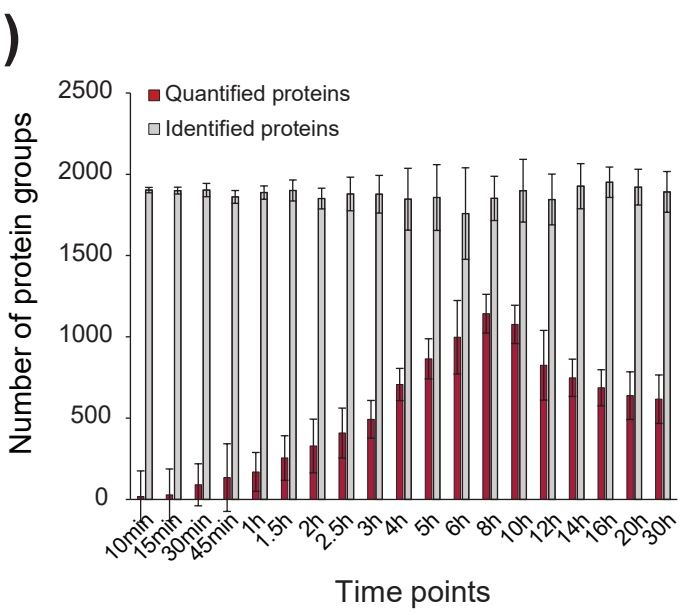

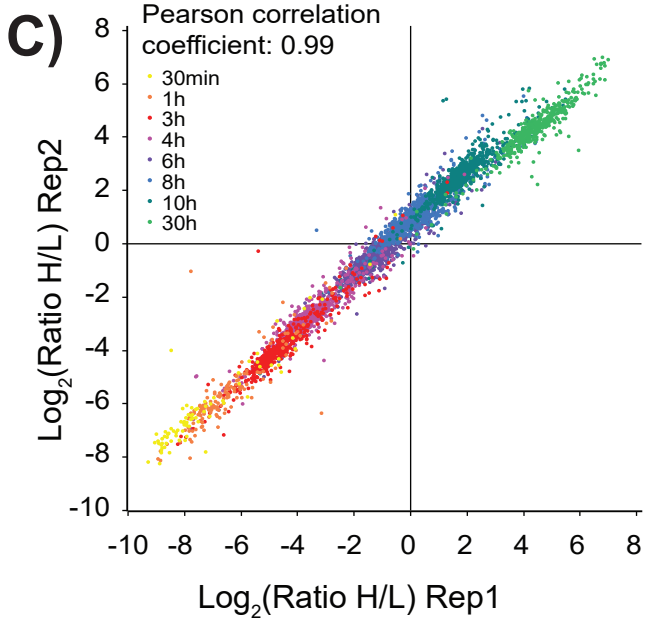

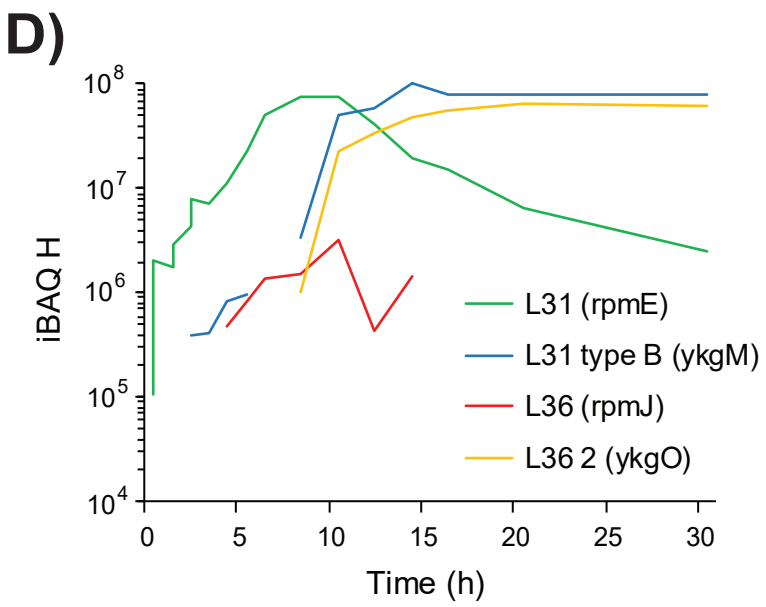

Suppl. Figure 3

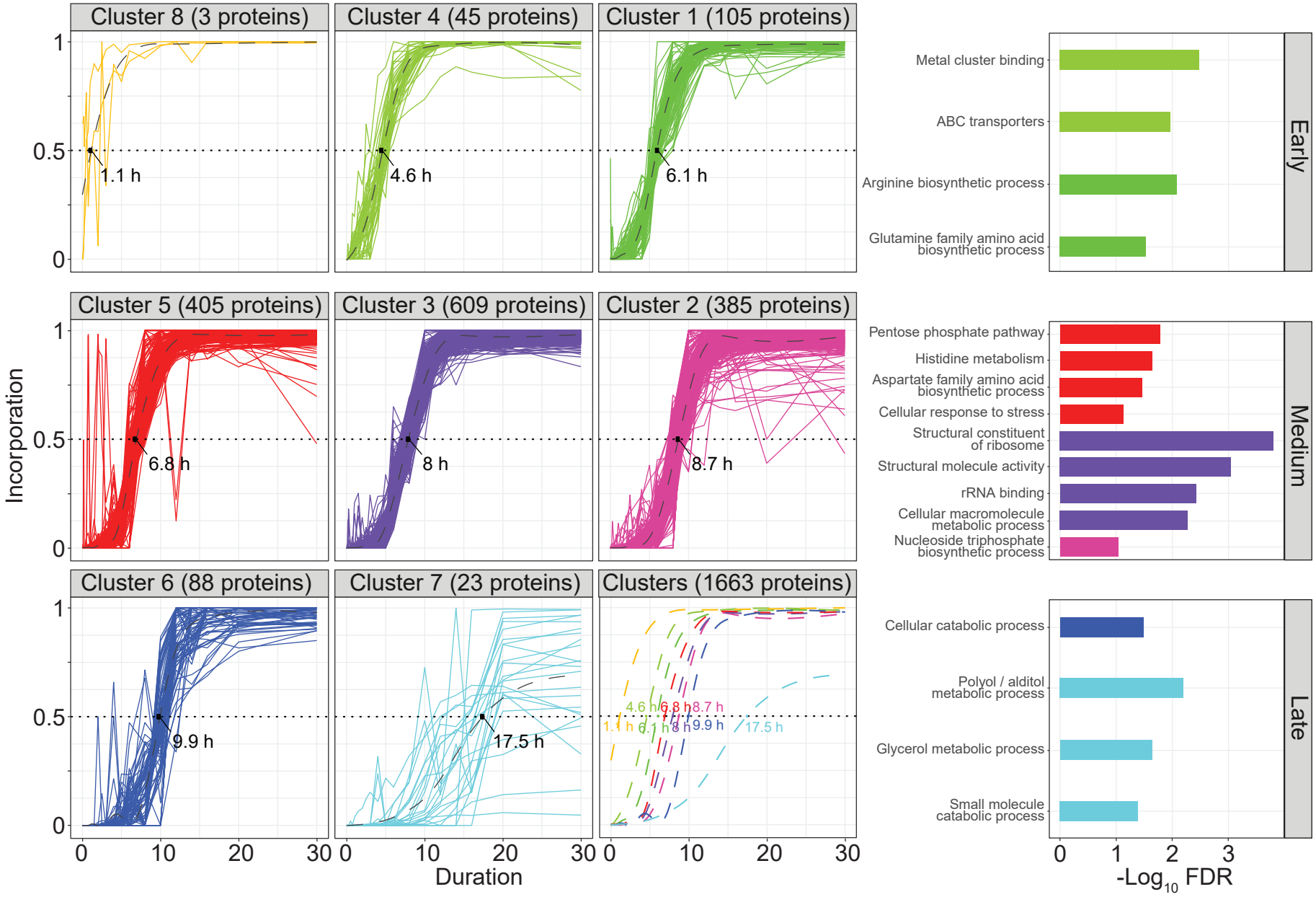

Suppl. Figure 4